Genomic and transcriptomic investigations of the evolutionary transition from oviparity to viviparity

Wei Gao[a,b,1], Yan-Bo Sun[a,1], Wei-Wei Zhou[a,1], Zi-Jun Xiong[a,c,1], Luonan Chen[d,e], Hong Li[f], Ting-Ting Fu[a,b], Kai Xu[a,b], Wei Xu[a,b], Li Ma[f], Yi-Jing Chen[f], Xue-Yan Xiang[c], Long Zhou[c], Tao Zeng[d], Si Zhang[d,g], Jie-Qiong Jin[a], Hong-Man Chen[a], Guojie Zhang[a,c,e,h], David M. Hillis[i,2], Xiang Ji[f,2], Ya-Ping Zhang[a,e,2], and Jing Che[a,e,j,2]

[a]State Key Laboratory of Genetic Resources and Evolution, Kunming Institute of Zoology, Chinese Academy of Sciences, 650223 Kunming, China; [b]Kunming College of Life Science, University of Chinese Academy of Sciences, 650204 Kunming, China; [c]China National Genebank, Beijing Genomics Institute-Shenzhen, 518083 Shenzhen, China; [d]Key Laboratory of Systems Biology, Center for Excellence in Molecular Cell Science, Institute of Biochemistry and Cell Biology, Chinese Academy of Sciences, University of Chinese Academy of Sciences, 200031 Shanghai, China; [e]Center for Excellence in Animal Evolution and Genetics, Chinese Academy of Sciences, 650223 Kunming, China; [f]Jiangsu Key Laboratory for Biodiversity and Biotechnology, College of Life Sciences, Nanjing Normal University, 210023 Nanjing, Jiangsu, China; [g]School of Life Science and Technology, ShanghaiTech University, 201210 Shanghai, China; [h]Section for Ecology and Evolution, Department of Biology, University of Copenhagen, DK-2100 Copenhagen, Denmark; [i]Department of Integrative Biology and Biodiversity Center, University of Texas at Austin, Austin, TX 78712; and [j]Southeast Asia Biodiversity Research Institute, Chinese Academy of Sciences, Yezin, 05282 Nay Pyi Taw, Myanmar

Contributed by David M. Hillis, December 11, 2018 (sent for review September 19, 2018; reviewed by Jonathan B. Losos and David D. Pollock)

Viviparous (live-bearing) vertebrates have evolved repeatedly within otherwise oviparous (egg-laying) clades. Over two-thirds of these changes in vertebrate reproductive parity mode happened in squamate reptiles, where the transition has happened between 98 and 129 times. The transition from oviparity to viviparity requires numerous physiological, morphological, and immunological changes to the female reproductive tract, including eggshell reduction, delayed oviposition, placental development for supply of water and nutrition to the embryo by the mother, enhanced gas exchange, and suppression of maternal immune rejection of the embryo. We performed genomic and transcriptomic analyses of a closely related oviparous–viviparous pair of lizards (*Phrynocephalus przewalskii* and *Phrynocephalus vlangalii*) to examine these transitions. Expression patterns of maternal oviduct through reproductive development of the egg and embryo differ markedly between the two species. We found changes in expression patterns of appropriate genes that account for each of the major aspects of the oviparity to viviparity transition. In addition, we compared the gene sequences in transcriptomes of four oviparous–viviparous pairs of lizards in different genera (*Phrynocephalus*, *Eremias*, *Scincella*, and *Sphenomorphus*) to look for possible gene convergence at the sequence level. We discovered low levels of convergence in both amino acid replacement and evolutionary rate shift. This suggests that most of the changes that produce the oviparity–viviparity transition are changes in gene expression, so occasional reversals to oviparity from viviparity may not be as difficult to achieve as has been previously suggested.

Phrynocephalus | viviparity | oviparity | convergent evolution | temporal–spatial expression

Viviparity (live-bearing) is a reproductive mode in which pregnant females maintain developing embryos inside their reproductive tracts and give birth directly to offspring (1). In contrast, oviparity (egg-laying) is the reproductive pattern in which females lay eggs that continue to develop independently of the mother until hatching. Viviparity evolves from oviparity through gradual increases in the length of egg retention until uterine embryogenesis is complete. Viviparous species provide an environment for embryonic development and protect the embryo from environmental threats. The transition between oviparity and viviparity has significant physiological and ecological consequences to the organisms and, as such, the processes involved in the transition are of general interest.

Squamate reptiles (lizards, snakes, and amphisbaenians) offer an ideal model system to study the evolutionary transition from oviparity to viviparity in vertebrates. About 20% of extant squamate species are viviparous. Viviparity has evolved between 98–129 times (depending on the analysis) in squamates, accounting for over two-thirds of all origins of viviparity in vertebrates (2–5). In addition, many of these origins of viviparity are evolutionarily recent, as viviparity has arisen in species or populations of otherwise oviparous clades. However, the phylogenetic timing of transitions from oviparity to viviparity is not always clear, and there are some suggestions of rare reversals from viviparity to oviparity in a few squamate groups; there are

Significance

The transition from oviparity to viviparity results in greater flexibility for parental control of embryonic development, which in turn allows viviparous organisms to reproduce successfully in otherwise adverse environments. These advantages have led to numerous origins of viviparity among vertebrates. We studied the genetic bases of this transition by comparing genomic and transcriptomic data of a closely related oviparous–viviparous pair of lizards (*Phrynocephalus przewalskii* and *Phrynocephalus vlangalii*). We identified genes whose temporal and spatial changes in expression account for the major physiological, morphological, and immunological aspects of the oviparity–viviparity transition. These changes account for eggshell reduction or degeneration, placental development, delayed oviposition, embryonic attachment, and inhibited maternal immune rejection of the embryo.

Author contributions: W.-W.Z., D.M.H., Y.-P.Z., and J.C. designed research; W.G., Y.-B.S., W.-W.Z., L.C., G.Z., D.M.H., X.J., Y.-P.Z., and J.C. managed the project; W.G., W.-W.Z., T.-T.F., K.X., W.X., J.-Q.J., and H.-M.C. conducted field work and performed DNA and RNA experiments; W.G., H.L., L.M., Y.-J.C., and X.J. carried out the breeding program and sample collection; Z.-J.X., X.-Y.X., L.Z., and G.Z. performed genome assembly and annotation; W.G., L.C., T.Z., and S.Z. identified genes related to placentation; W.G. and Y.-B.S. performed the analysis of convergent evolution; Y.-B.S. performed the analysis of positive selection; W.G. performed transcriptomic expression analysis; and W.G., Y.-B.S., D.M.H., X.J., Y.-P.Z., and J.C. discussed results and wrote the paper.

Reviewers: J.B.L., Washington University in St. Louis; and D.D.P., University of Colorado Health Sciences Center.

Conflict of interest statement: D.D.P. and G.Z. are coauthors on a 2014 paper.

Data deposition: The data have been deposited in the Genome Sequence Achieve, gsa.big.ac.cn (accession no. CRA001096). The whole-genome sequence data reported in this paper have been deposited in the BIGD Genome Warehouse, bigd.big.ac.cn/gwh (accession nos. GWHAAFC00000000 and GWHAAFD00000000) and are also available in the CNGB Nucleotide Sequence Archive, https://db.cngb.org/cnsa (accession no. CNP0000203).

[1]W.G., Y.-B.S., W.-W.Z., and Z.-J.X. contributed equally to this work.

[2]To whom correspondence may be addressed. Email: chej@mail.kiz.ac.cn, zhangyp@mail.kiz.ac.cn, jixiang@njnu.edu.cn, or dhillis@austin.utexas.edu.

This article contains supporting information online at www.pnas.org/lookup/suppl/doi:10.1073/pnas.1816086116/-/DCSupplemental.

nonetheless many cases in which the recent transition from oviparity to viviparity is strongly supported (4–9). Comparative studies of closely related oviparous and viviparous species has confirmed that this transition in parity requires a number of physiological, morphological, and immunological changes. These include reduced eggshell (10–12), delayed oviposition (11, 13, 14), placental development for supply of water and nutrition to the embryo by the mother (13, 15, 16), enhanced gas exchange (14, 15, 17), and suppression of maternal immune rejection of the embryo (18, 19). However, the specific changes to genes or their expression that result in these major transformations are largely unknown.

Recently, a comparative analysis based on restriction-site–associated DNA data in *Zootoca vivipara*, a species with both oviparous and viviparous populations, showed that several gene mutations may be related to morphological changes of the uterus associated with viviparity (20). Furthermore, by comparing transcriptomic data of the uterus between pregnant and nonpregnant female *Chalcides ocellatus*, Brandley et al. (21) identified numerous differently expressed genes that are potentially related to nutrient provision to the embryo, uterus remodeling for placentation, and immune system regulation. Some of the same genes identified by Brandley et al. (21) also exhibited expression changes between an oviparous–viviparous pair of distantly related species (22). However, the lack of gene-expression profiles across different developmental stages, especially comparing a closely related oviparous–viviparous pair of species or populations, limits our understanding of how expression changes through development may control the oviparity–viviparity transition.

To further study the genetic and expressional basis of these changes from oviparity to viviparity, we compared genomic and transcriptomic data between two *Phrynocephalus* species (Agamidae) with different reproductive modes. Six currently recognized viviparous species of *Phrynocephalus* are distributed on the Qinghai-Tibetan Plateau and its margins (23), and consist of a closely related monophyletic group within an otherwise oviparous clade of lizards. The divergence time of the viviparous species from their oviparous relatives was about 13.5 Ma (24). In our study, we compared the viviparous *Phrynocephalus vlangalii* to the oviparous *Phrynocephalus przewalskii*. We sequenced and compared the genomes of both species, and compared the transcriptomes of maternal oviducts through the development of eggs and embryos. In particular, we compared the expression pattern of genes that are involved in shell gland development, egg retention, embryo attachment, placenta development, and immune tolerance. We further compared the transcriptomes of three other pairs of closely related oviparous and viviparous species of the genera *Eremias*, *Scincella*, and *Sphenomorphus* to examine potential sequence convergence associated with viviparity across independent origins of this transition.

Results and Discussion

Genome Sequencing and Gene Annotation. We generated 174 Gb of high-quality reads for *P. przewalskii* (with genome size 1.84 Gb) and 232 Gb of high-quality reads for *P. vlangalii* (with genome size 1.98 Gb). Although both species have relatively high heterozygosity as assessed by *k*-mer analysis (*P. przewalskii*: 1.4%; *P. vlangalii*: 0.6%), our final assemblies were still of high quality (contig and scaffold N50 values for *P. przewalskii*: 56.4 kb and 6.88 Mb for *P. vlangalii*: 31.2 kb and 2.39 Mb) (*SI Appendix*, Table S1), which covered about 95% (1.76 of 1.84) of the *P. przewalskii* genome and 92% (1.82 of 1.98) of the *P. vlangalii* genome. About 97% of both assemblies were sequenced to >10× coverage. The average GC content was about 43% for both genomes (*SI Appendix*, Fig. S1), similar to other vertebrates (*SI Appendix*, Fig. S2), indicating that our assemblies were not strongly affected by GC-biased sampling.

Multiple approaches for gene prediction identified 21,937 and 22,994 protein-coding genes, with average coding sequence length of 1,415 bp for *P. przewalskii* and 1,388 bp for *P. vlangalii* (*SI Appendix*, Table S2). More than 99% of the protein-coding genes of both species were functionally annotated according to SwissProt and TrEMBL databases (*SI Appendix*, Table S3). Using the BUSCO database of 3,023 universal single-copy orthologs found across vertebrates (25), we sequenced 84.4% and 87.5% of the expected vertebrate genes in *P. przewalskii* and *P. vlangalii*, respectively (*SI Appendix*, Table S4).

Gene-Expression Changes During Uterine Embryogenesis. We evaluated gene expression in the oviduct (Fig. 1*A*) by sequencing the transcriptomes of oviducts from preovulation to postoviposition (for the oviparous species) or postparturition (for the viviparous species). Principal components analysis (PCA) of all orthologous genes (n = 16,451 genes) shows major differences in gene-expression changes through the reproductive development of the two species (Fig. 1*B*). The first component explained 51.3% of the variance and the second explained 13.1%. In both species, gene expression at S1 (the ovarian egg stage) is markedly different from gene expression postovulation. In addition, in both species, gene expression through S2 and S3 (after ovulation, but before egg-laying) is relatively constant (compared with expression changes between other stages). However, this relative stasis of gene expression continues in the viviparous species through birth, as opposed to the rapid and sudden shift in gene expression in the oviparous species at egg-laying (Fig. 1*B*). This suggests that viviparous species may prolong uterine embryogenesis, at least in part, by delaying or avoiding a sudden shift in gene-expression patterns.

We identified numerous differentially expressed genes (DEGs) during uterine embryogenesis of both species (Fig. 1*C*). The viviparous species (*P. vlangalii*) exhibited considerably more up-regulation of genes than did the oviparous species (*P. przewalskii*) in the postovulation stages (when contrasted with S1). In addition, the oviparous species exhibited considerably more down-regulation of genes in these periods than did the viviparous species (Fig. 1*C*). In the oviparous species, most genes quickly returned to preovulation gene-expression levels after oviposition, whereas in the viviparous species, many genes still showed significant changes in expression level between S1 (preovulation) and S6 (after birth) (Fig. 1*C*). The number of DEGs in each period compared with expression levels in the previous period shows the smallest change in expression between S2 and S3 in *P. przewalskii* (Fig. 1*C*), which was consistent with the results of the PCA (Fig. 1*B*). In *P. vlangalii*, more genes are up-regulated at S3 compared with S2 and more genes down-regulated at S4 compared with S3, indicating more considerable changes in S3 in the viviparous species compared with the oviparous species (Fig. 1*C*). We detected stage-specific highly expressed genes (HEGs) at every period, but S3 in the viviparous species exhibited by far the greatest number (383) of HEGs (*SI Appendix*, Fig. S3). Considering that S3 in *P. vlangalii* corresponds to the stage just before egg-laying in *P. przewalskii*, these numerous HEGs in S3 of the viviparous species suggest a likely explanation for physiological or morphological changes (e.g., egg retention and placental development) in the viviparous *P. vlangalii*.

Eggshell Gland Degeneration. One important step for the evolution of viviparity in squamates involves eggshell reduction (10), which allows a closer association of uterine and embryonic tissues and promotes maternal–fetal gas exchange (11) or maternal recognition (12, 26). A significant reduction in eggshell thickness or loss of the eggshell has been observed in virtually all viviparous species (26), and the reason can be attributed to the degeneration or reduction of uterine shell glands. In squamates, shell glands undergo seasonal changes associated with the reproductive cycle and are formed primarily during vitellogenesis; the glands then regress following ovulation (10). Our analysis of the

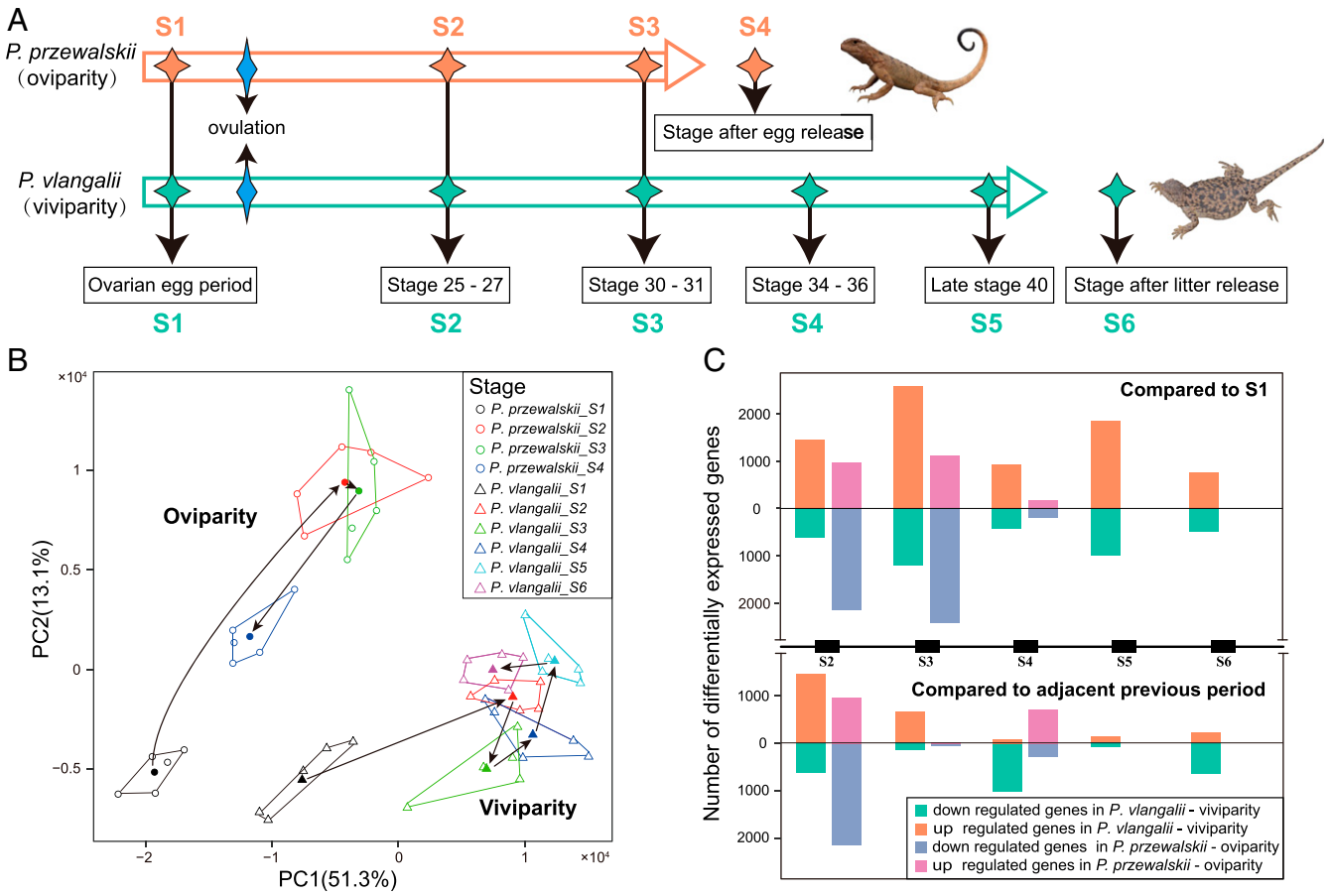

Fig. 1. Gene-expression pattern and changes of two species of *Phrynocephalus* through their respective reproductive cycles. (*A*) Sample collection relative to the reproductive cycles. The reproductive stages of the oviparous species *P. przewalskii* are represented in orange, and those of the viviparous species *P. vlangalii* are represented in green. (*B*) PCA of gene expression through the reproductive cycles of *P. przewalskii* (circles), and *P. vlangalii* (triangles). Hollow symbols represent the individual values for each sample and solid symbols represent the average values for each species at each stage. Arrows indicate the time course of the reproductive cycle. (*C*) Number of DEGs in pairwise comparisons between each reproductive period. The *Upper* half illustrates the number of differentially expressed genes in each period compared with S1; the *Lower* half shows the number of DEGs in each period compared with the previous period.

stage-specific HEGs in S1 suggests a clear mechanism for eggshell degeneration in viviparous squamates.

The earliest changes in the transition from oviparity to viviparity are expected in S1, when an eggshell gland is expressed in egg-laying species, whereas it is absent or reduced in viviparous species. We identified 148 S1-specific HEGs (Fig. 2*A* and *SI Appendix*, Table S5) in *P. przewalskii* (oviparous), among which we would expect the genes responsible for the shell gland formation. Gene Ontology (GO) enrichment analysis of these genes (*SI Appendix*, Fig. S4 and Table S6) showed that many of these genes are involved in a response to growth factor, cell differentiation, proliferation and morphogenesis, secretion and transport vesicle, and protein synthesis and localization, each of which are closely related to the formation of a shell gland (Table 1).

To investigate how many of these S1-specific HEGs of the oviparous *P. przewalskii* could be involved in shell gland formation, we examined the expression patterns of these same genes at S1 in the viviparous *P. vlangalii*. Only 3 of these 148 S1-specific HEGs were also highly expressed in S1 of *P. vlangalii* (Fig. 2 *A* and *B*), suggesting that the loss of an egg-shell gland in the viviparous species may involve expression changes in dozens of genes.

Estrogens are essential for normal oviduct growth and oviduct hypertrophy; increases in the number and size of shell glands are observed when oviducts are exposed to exogenous 17β-estradiol (E2) in reptiles (27, 28). The estrogen-induced growth factors, such as insulin-like growth factor (IGF1) and epidermal growth factor (EGF), may mediate the effect of E2 in shell gland formation (27). We found that the estrogen receptor genes *ESR1* and *ESR2* were highly expressed at S1 in *P. przewalskii*, but not in *P. vlangalii* (Fig. 2*C* and *SI Appendix*, Table S14), consistent with their reported role. Similarly, the genes encoding two growth factors, *IGF1* and *EGF*, together with their receptors, were also highly expressed at S1 in *P. przewalskii*, whereas and the expression of *IGF1* and *EGF* were nearly undetectable in *P. vlangalii* (Fig. 2*C* and *SI Appendix*, Table S14). These specific expression-pattern changes appear to be among the changes associated with the loss of eggshell formation in the viviparous species.

Embryo Attachment and Placenta Development. The development of a placenta is another important step in the evolution of viviparity, as a placenta is needed to provide the embryo with water and nutrients, and to provide gas exchange. In viviparous squamates, two types of placentae begin to develop at the middle periods of gestation: a chorioallantoic placenta on the embryonic pole and a yolk-sac placenta on abembryonic pole (29–31). Most placentae of viviparous squamates (including *P. vlangalii*) are formed via close appositions of uterine and embryonic tissues; the embryonic tissues do not breach or invade uterine epithelia, and thus these species have very simple placentae (17). Even so, the dramatic remodeling of uterine epithelium still occurs during pregnancy as the placenta develops (31).

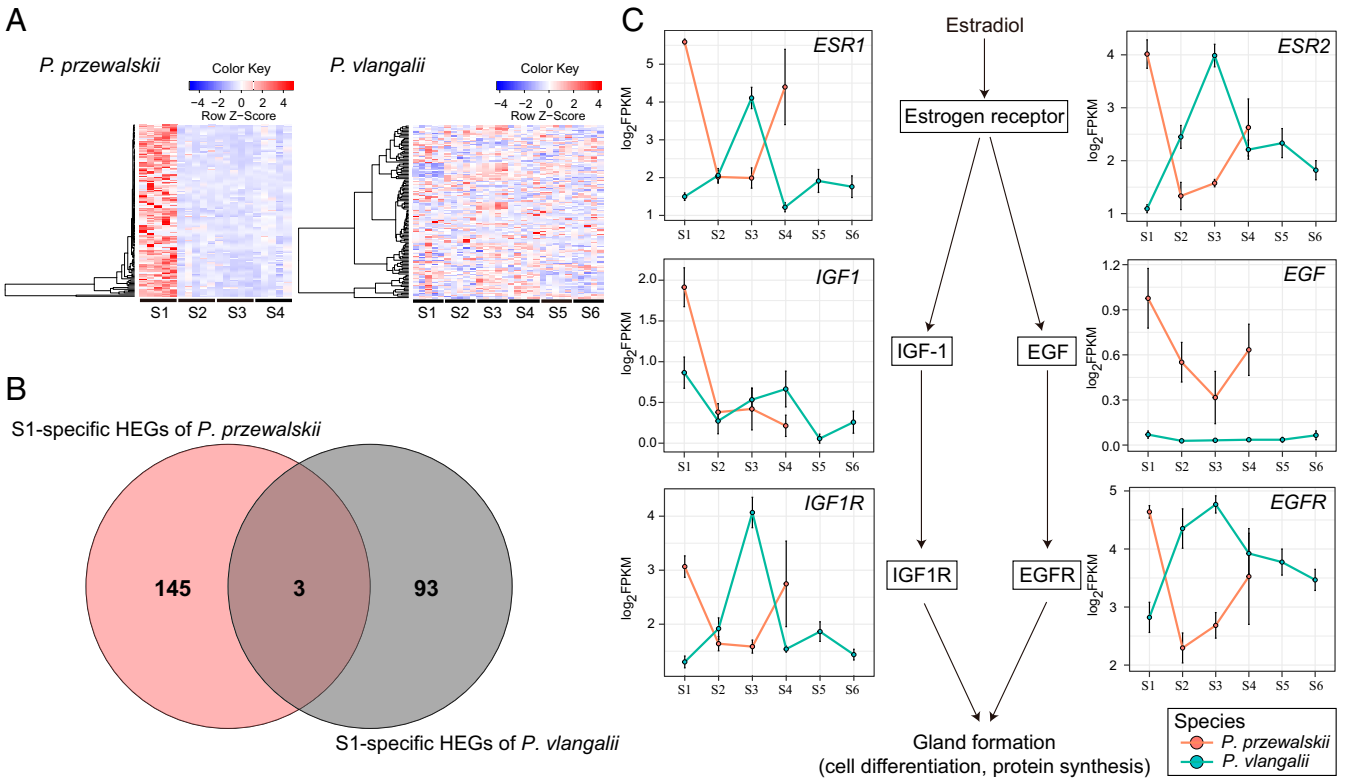

Fig. 2. Expression pattern of genes related to shell gland degeneration. (*A*) Expression heatmaps of genes specifically highly expressed at S1 in *P. przewalskii* (*Left*) and orthologous genes in *P. vlangalii* (*Right*). (*B*) Comparison of genes specific highly expressed before ovulation (at S1) of two species. (*C*) Expression pattern of key genes that are related the expression of shell glands. Red lines and circles represent gene-expression in *P. przewalskii*, green lines and circles represent gene-expression in *P. vlangalii*. Error bars present ±1 SE.

A few candidate genes/functions have been reported as being associated with development of the placenta, including the gene *Hβ58* (32), estrogen-driven phosphorylation of effector proteins (13), and protease enzymes (20). In addition, adhesion mechanisms are necessary to keep the uterine and embryonic components adjacent during placental development and throughout subsequent gestation periods (17), during which cadherins are a potential mechanism of embryonic attachment in viviparous reptiles (as in the genus *Niveoscincus*) (33).

Placental development occurs during the middle stages of gestation (30, 31). To test whether the genes and functions that have been reported to be associated with placentation show consistent expression patterns in our studied viviparous species (*P. vlangalii*), as well as to identify additional genes that may be associated with placentation, we looked for stage-specific HEGs at midgestation periods of *P. vlangalii* (when the placenta begins to develop) that were not highly expressed at any periods of egg/embryo development in *P. przewalskii*. Using this strategy, we found 481 candidate genes that may be involved in placenta development in the viviparous species (*SI Appendix*, Table S7). These genes fall into six patterns of expression, from S1 to S5, which we labeled patterns P1–P6 (Fig. 3*A*). Pattern class P5 (high expression at S3) was by far the most common pattern observed (429 of 481) (Fig. 3*A*). GO analysis of the 481 candidate genes showed many functions that can affect uterine epithelial structure changes, and almost all genes enriched in these functions belong to pattern class P5 (Table 1 and *SI Appendix*, Fig. S5 and Table S8). Among them, the functions associated with proteolysis are likely involved in extracellular matrix degradation before the remodeling of the endometrium (20, 21, 34). Another important finding is that the functions associated with cell differentiation and cell polarity establishment showed specific high expression in S3 (Table 1), suggesting their roles in the remodeling of the uterus.

There are also some highly expressed genes associated with the steroid hormone-mediated signaling pathway (GO:0043401), estrogen receptor activity (GO:0030284), and the transforming growth factor β-receptor signaling pathway (GO:0007179) (Table 1). These changes suggest that steroid hormones and growth factors are involved in regulating uterine changes during placentation. There are also some up-regulated genes associated with adhesion functions, such as regulation of cell–cell adhesion mediated by cadherin (GO:2000047), positive regulation of cell adhesion (GO:0045785), and integrin αv-β8 complex (GO:0034686) (Table 1). These results further highlight the potential roles of adhesion in embryo attachment to the maternal uterus during placental development.

Considering the large number of genes that are highly expressed at S3 of *P. vlangalii* (pattern P5), and the close association of the reported functions of these genes with placental development and function, S3 appears to be the stage of placentation in *P. vlangalii*. We therefore analyzed which genes had highly correlated expression with developmental stage S3 using weighted gene correlation network analysis (WGCNA). This analysis identified a module that is colored in blue in Fig. 3*B* [$r = 0.72$, false-discovery rate (FDR) = 0.00025] (*SI Appendix*, Fig. S6 and Table S9). Enrichment analysis of genes with a probability of membership in this module of at least 0.9 (*SI Appendix*, Fig. S7) showed that most of them exhibit functions associated with uterine epithelial structure changes (*SI Appendix*, Fig. S8 and Table S10).

We constructed an expression network of genes that belong to expression pattern P5 in the "blue module," and retained genes with an edge weight in this network of greater than 0.5 (Fig. 3*C*). The resulting network contained 206 genes; we selected the 20 with the highest degree of connectivity as hub genes (Fig. 3*C*

Table 1. Candidate GO terms associated with functions involved in viviparity

Source and function	Category	*P* value	No.	Term
Group A	GO:0002065	0.0029	3	Columnar/cuboidal epithelial cell differentiation
	GO:0045597	0.0038	12	Positive regulation of cell differentiation
	GO:0045176	0.0045	2	Apical protein localization
	GO:0036120	0.0047	2	Cellular response to platelet-derived growth factor stimulus
	GO:0022604	0.0048	10	Regulation of cell morphogenesis
	GO:0043567	0.0086	2	Regulation of insulin-like growth factor receptor signaling pathway
	GO:0050673	0.0135	3	Epithelial cell proliferation
	GO:0030133	0.0283	3	Transport vesicle
	GO:0060562	0.0337	3	Epithelial tube morphogenesis
	GO:0032252	0.0378	1	Secretory granule localization
Group B	GO:0042127	0.0004	45	Regulation of cell proliferation
	GO:0043401	0.0011	6	Steroid hormone mediated signaling pathway
	GO:0030284	0.0035	2	Estrogen receptor activity
	GO:0007179	0.0040	8	Transforming growth factor beta receptor signaling pathway
	GO:0030856	0.0042	8	Regulation of epithelial cell differentiation
	GO:0051603	0.0045	20	Proteolysis involved in cellular protein catabolic process
	GO:2000114	0.0058	4	Regulation of establishment of cell polarity
	GO:0043161	0.0080	11	Proteasome-mediated ubiquitin-dependent protein catabolic process
	GO:0034329	0.0122	11	Cell junction assembly
	GO:0032878	0.0143	4	Regulation of establishment or maintenance of cell polarity
	GO:0031532	0.0312	5	Actin cytoskeleton reorganization
Group C	GO:2000047	0.0046	2	Regulation of cell–cell adhesion mediated by cadherin
	GO:0045785	0.0386	12	Positive regulation of cell adhesion
	GO:0034686	0.0440	1	Integrin αv-β8 complex

Source and function: group A, GO terms of S1-specific HEGs in *P. przewalskii*, related to eggshell gland development; group B, GO terms of midgestation period-specific HEGs in *P. vlangalii*, related to placentation; group C, GO terms of midgestation period-specific HEGs in *P. vlangalii*, related to embryo attachment.

and *SI Appendix*, Table S11). Notably, the two genes that encode estrogen receptors, *ESR1* and *ESR2*, were identified as hub genes in this module (*SI Appendix*, Fig. S7), which is consistent with the key roles of these receptors in regulating uterine epithelium changes (14). Among these hub genes, estrogen receptor (*ESR1*), together with two growth factor receptors (*GHR* and *IGF1R*), appear to play key roles in initiating the uterine changes during placentation of *P. vlangalii*. In addition, genes *KRT80*,

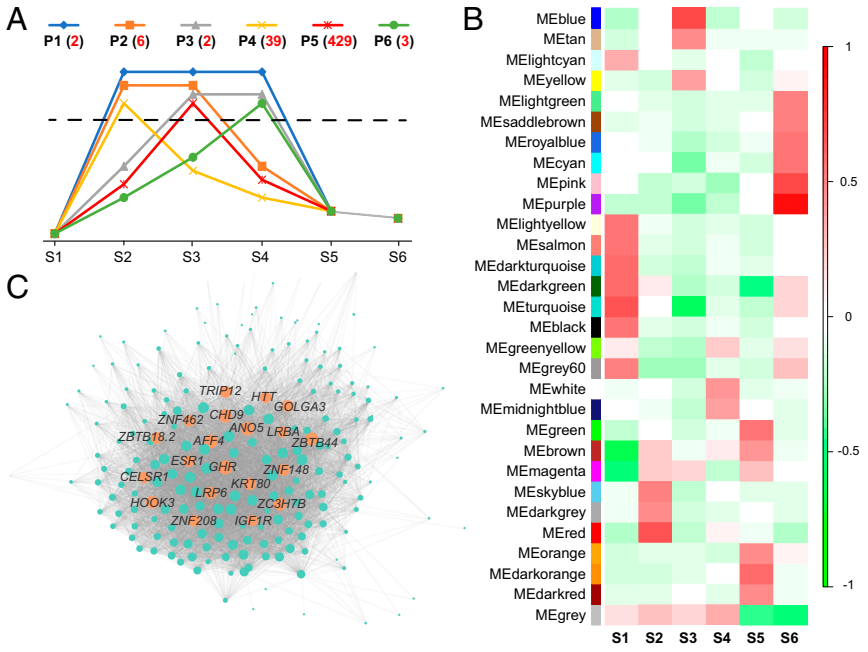

Fig. 3. Gene-expression patterns involved in embryo attachment and placental development. (*A*) Gene-expression patterns of genes highly expressed at midgestation of *P. vlangalii*. The numbers in parentheses after each pattern indicates that number of genes that exhibit the respective pattern. (*B*) Module–period relationships in *P. vlangalii* according to the WGCNA analysis. The color indicates the respective correlation coefficient, as shown in the scale bar. (*C*) Coexpression network of P5 genes that are found in "blue module." Edges with weight >0.5 are plotted. Circle sizes represent the degree of each gene in the network. Orange dots represent the top 20 most connected genes in this network; other genes are represented by blue dots.

LRP6, and *HOOK3* are likely to be involved in promoting uterine cell differentiation (35, 36). One gene encoding a receptor of cadherins, *CELSR1*, is likely related to the attachment of the embryo to maternal tissue during placentation (37).

Estrogen (together with its receptors) is a major regulator of oviduct/uterine plasticity in many vertebrates (38–40). Estrogen is involved in seasonal enlargement of oviducts in some reptiles (39, 41, 42). The differential gene-expression pattern of estrogen receptor-related genes in oviparous and viviparous species is associated with the structural transition from oviparity to viviparity. The high expression of *ESR1* and *ESR2* at the ovarian egg stage supports their role in shell gland development in oviparous *P. przewalskii*. The expression of these genes shifts to midgestation in the viviparous *P. vlangalii*, at the same time the placentae form. Thus, the timing and location of expression of estrogen receptors appear to play important roles in structural changes that are required for viviparity.

Egg Retention. The evolution of viviparity requires prolonged egg retention until embryogenesis is complete (13, 14). Oviposition/birth is accomplished through periodic muscle contraction, and several hormones are known to play a role in stimulating these contractions, especially the hormones arginine vasotocin (AVT) and prostaglandins (PGs) (43–46). AVT is an oligopeptide that is homologous to oxytocin in placental mammals, where it promotes muscle contraction during parturition (47). It is also known to stimulate uterine contractions in both oviparous and viviparous species (43, 48, 49). In this study, gene set enrichment analysis (GSEA) (*SI Appendix*, Fig. S9) showed that the oxytocin-signaling pathway was significantly up-regulated at S5 (late stage 40 before parturition) compared with S4 (enrichment score = 0.39817, FDR = 0.03052) in *P. vlangalii*, and also compared with S1 (enrichment score = 0.36377, FDR = 0.03494). The receptor for AVT, mesotocin receptor (MTR), was slightly but not significantly up-regulated at S5 compared with S4, but was significantly up-regulated at S5 compared with S1 (Fig. 4*A* and *SI Appendix*, Table S14). However, the period of highest expression for *MTR* was at S3. In contrast, we found no significant differences of expression in the oxytocin-signaling pathway between S3 (before oviposition) and any other periods in *P. przewalskii* (*SI Appendix*, Fig. S10). Hormones of another family, PGs, increase in concentrations in plasma at the time of oviposition or birth, and are associated with the onset of labor in eutherian mammals, as well as uterine contraction in reptiles (43–45). PTGS2, the key enzyme for PG synthesis (50), was significantly up-regulated during all gestation stages compared with S1 in *P. przewalskii* (Fig. 4*B* and *SI Appendix*, Table S14). Expression of *PTGS2* peaked at S3, and then dramatically dropped after egg release (S4) in this oviparous species (Fig. 4*B* and *SI Appendix*, Table S14). By comparison, there was similar expression pattern of *PTGS2* from S1 to S3 in *P. vlangalii*, with less reduction in S4 and S5, followed by dramatic reduction in expression after parturition (Fig. 4*B* and *SI Appendix*, Table S14).

Inhibitors or antagonists for AVT and PGs may play an important role in prolonging egg retention. For example, progesterone (P4), an inhibitor of AVT, which is secreted primarily by the corpus luteum, is associated with uterine quiescence in reptiles (48). In this study, we found that the autonomic nervous system seems to play a more important role in pregnancy maintenance through inhibiting the role of PGs by uterine β-2-adrenergic receptor (ADRB2) (43, 51). The expression of *ADRB2* was significantly up-regulated after pregnancy compared with the preovulation period in *P. vlangalii*, gradually rising along with pregnancy until S5, and then dramatically decreasing at S6 (Fig. 4*C* and *SI Appendix*, Fig. S11 and Table S14).

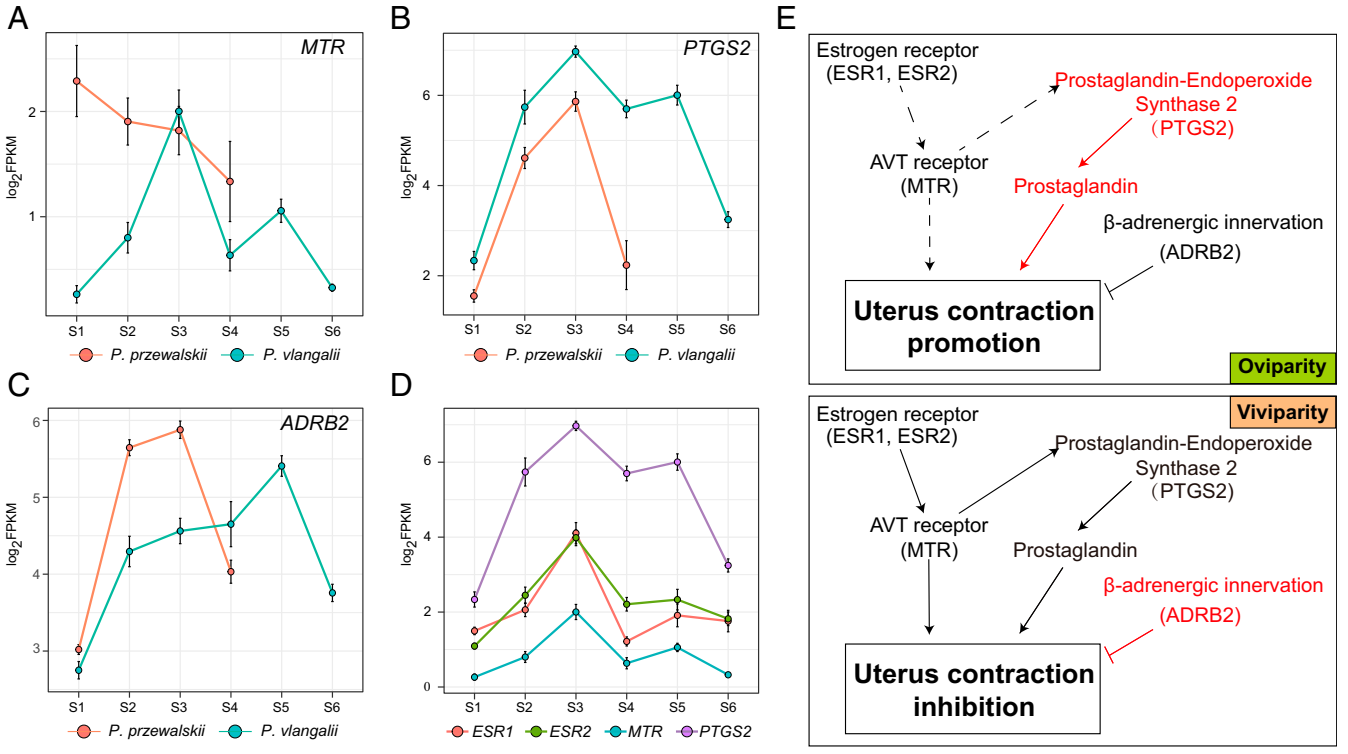

Fig. 4. Gene-expression patterns related to egg retention. (*A*) Gene-expression pattern of the AVT receptor (MTR). (*B*) Gene-expression pattern of the key enzyme for PG synthesis (PTGS2). (*C*) Gene-expression pattern of β-2-adrenergic receptor (ADRB2). Red lines and circles represent gene-expression in *P. przewalskii*, green lines and circles represent gene-expression in *P. vlangalii*. Error bars indicate ±1 SE (*D*) Similar gene-expression pattern of gene *PTGS2*, *MTR*, *ESR1*, and *ESR2*. Error bars indicate ±1 SE. (*E*) Differences between the oviparous and viviparous species related to egg retention at S3 and S4. Red text represents up-regulated functions and black text represents down-regulated functions. Dashed lines indicate that the corresponding function may have been lost.

Similarly, *ADRB2* was also up-regulated after pregnancy, but in contrast down-regulated after S3, and there were no significant differences in expression between S2 and S3 in *P. przewalskii* (Fig. 4*C* and *SI Appendix*, Fig. S11 and Table S14). Thus, uterine β-adrenergic innervation appears to function in maintaining muscle quiescence during gestation in *Phrynocephalus*, and the differential expression pattern of *ADRB2* in *P. vlangalii* compared with *P. przewalskii* appears to allow embryo retention in *P. vlangalii*.

Taken together, the differential expression patterns of key genes related to oviposition and parturition explain the embryonic retention in the viviparous species (Fig. 4*E*). The specific high expression of *PTGS2* at S3 may induce oviposition in *P. przewalskii* and the significant down-regulation of *ADRB2* at S4 supports its role in maintaining uterine quiescence. The primary changes in *P. vlangalii* are that *PTGS2* is down-regulated after S3 (at S4), which reduces the facilitating factor of uterine contraction, whereas *ADRB2* is continuously highly expressed after S3, which increases the inhibition of uterine contraction (Fig. 4*E*). This provides an explanatory mechanism for embryonic retention in the viviparous *P. vlangalii*. The expression of *PTGS2* may be induced in different ways in the two species. The estrogen receptor can induce the expression of the AVT receptor (52), and thereby promote the expression of *PTGS2*. The gene-expression pattern of these three factors was very similar (Fig. 4*D*) and the reduction of *PTGS2* at S4 may be caused by the down-regulation of the estrogen receptor in *P. vlangalii*. In contrast, there are no obvious correlations between expression of these genes in *P. przewalskii*.

Convergent Evolution Across Viviparous Lizards. Many parallel origins of viviparity in squamates have been accompanied by repeated convergence of physiological and morphological changes. Many of these convergent changes have likely been achieved through changes in gene expression, similar to those discussed above for *Phrynocephalus*. Have these convergent changes in physiology and morphology also been accompanied by specific convergent changes in the sequences of genes and proteins? To examine this question, we selected three additional pairs of lizards, each of which included two congeneric species with different reproductive modes (Fig. 5*A*) and sequenced the transcriptome of a single pooled RNA library from heart, liver, lung, muscle, brain, and oviduct for each species. We compared 9,118 orthologous genes among these four species pairs of the genera *Eremias*, *Phrynocephalus*, *Scincella*, and *Sphenomorphus* (Fig. 5*A*). Convergence in the genes was calculated by examining convergent amino acid replacements (53) and convergent shifts in evolutionary rate (54).

In the convergent amino acid replacement analysis, only four genes (*C7*, *NKTR*, *NBEAL2*, *PTX2*) were detected that experienced amino acid replacements at the same positions in all four viviparous species (*SI Appendix*, Table S12), a level of convergence that can be achieved by chance with frequency of 11.6% (116 of 1,000) (Fig. 5*B*). But considering these genes' function in the immune regulation (55–58) and expression patterns (Fig. 5 *C* and *D* and *SI Appendix*, Table S14), we cannot rule out their important role in regulating the immune response to accommodate attachment of the embryo in the oviparity–viviparity transition.

This low level of observed sequence convergence was further supported by our analysis of convergent shifts in evolutionary rates (53). No genes exhibited convergent changes in evolutionary rates across viviparous species in our analysis after multiple test correction (*SI Appendix*, Table S13). However, this test is dependent on the number of species examined, and a larger sample of viviparous species may identify more convergent evolutionary rate shifts associated with the evolution of viviparity (53).

Conclusions. Expression patterns of oviducts during uterine embryogenesis differed markedly between oviparous and viviparous species. We found changes in expression patterns of appropriate genes that account for each of the major aspects involved in the transition from oviparity to viviparity, including eggshell reduction, embryo attachment, placental development, egg retention, and immune tolerance. Several genes related to regulating immune responses during gestation experienced convergent amino acid replacements in all four viviparous species examined in this study.

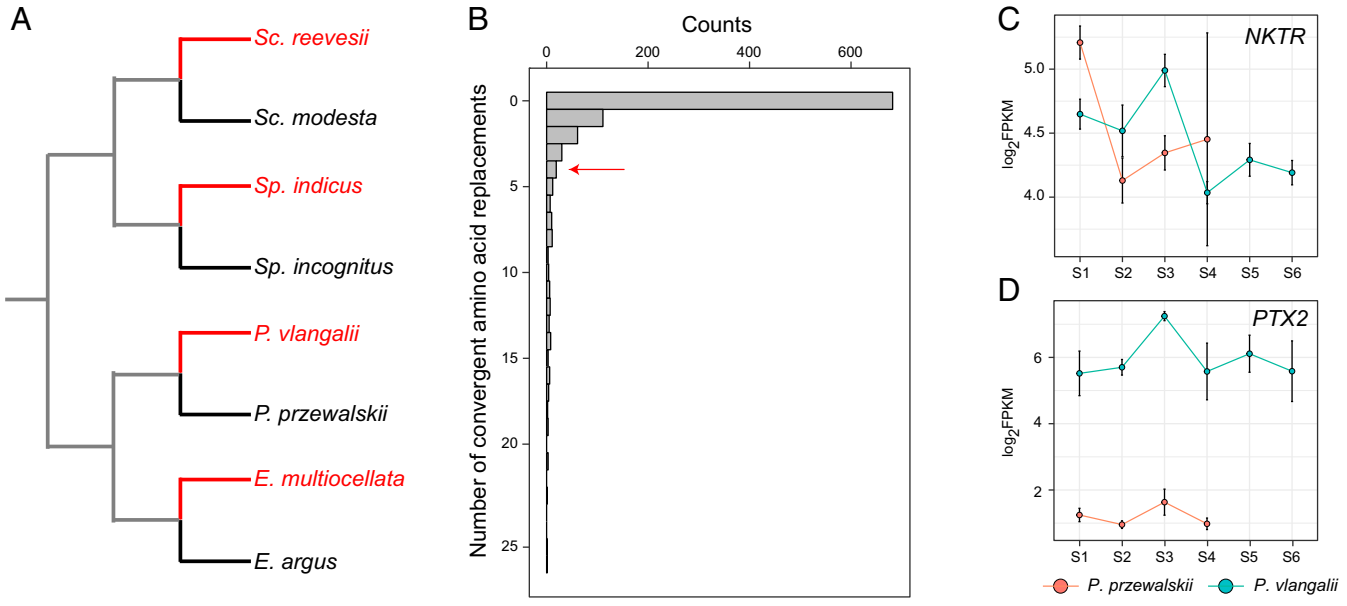

Fig. 5. Convergent sequence evolution in viviparous lizards. (*A*) Phylogenetic relationships of species examined in the convergence analysis (branch lengths are arbitrary). Red names indicate viviparous species and black names indicate oviparous species. (*B*) The number of convergent amino acid replacements observed across four viviparous species in the simulations. Red arrow showed the position of observed number in viviparous lizards. (*C* and *D*) Gene-expression patterns of *NKTR* (*C*) and *PTX2* (*D*), two genes that exhibited convergent amino acid replacements in their encoded proteins at same position across all four viviparous species. Red lines and circles represent gene-expression in *P. przewalskii*, green lines and circles represent gene-expression in *P. vlangalii*. Error bars indicate ±1 SE.

However, the vast majority of the changes we observed (among the genes likely to be associated with the transition from oviparity to viviparity) are changes in the expression levels and expression timing of genes, rather than in gene sequences. We examined the evidence for positive selection of genes on the branch leading to *P. vlangalii*, and detected only 60 genes that exhibit signatures of positive selection (*SI Appendix*, Fig. S12). None of these genes had any clear functional role in reproduction. Therefore, it appears that most of the changes needed in the transition from egg-laying to viviparity occur through up- or down-regulation of genes. If the genes themselves experience minimal substitutional changes, then the evolutionary reversal from viviparity to oviparity may not be as difficult to achieve, as has been thought to date (7, 8). Indeed, there are three genera of reptiles in which there is relatively strong evidence to support a reversal from viviparity back to oviparity: in *Lachesis*, *Eryx*, and *Liolaemus* (5). Integrative studies of transcriptomes, morphology, and ecology of these three cases are needed to shed light on the possible reversals, the mechanisms that result in reversal, and the ecological conditions under which reversal in parity mode is favored.

Materials and Methods

Genome Sequencing, Assembly, and Annotation. Genomic DNA from male *P. przewalskii* and *P. vlangalii* was extracted from muscle tissue, and eight paired-end DNA libraries with different insert size lengths (170 to 40 kb) were constructed. All of the sequences were generated via the Illumina HisEq 2000/2500 platform, and were then assembled by Platanus (59). The completeness of each assembly was evaluated with BUSCO pipeline (25). The protein-coding genes were predicted by utilizing three different methods: homology-based, ab initio, and RNA-sequencing–based predictions. Ortholog genes of these two species were calculated using the method OrthoFinder (60). Additional details of the genome assembly are given in *SI Appendix*.

Collection of Tissues Across Developmental Stages. Adult females of *P. vlangalii* were collected from Dulan, Qinghai, China; adult females of *P. przewalskii* were collected from Jingtai, Gansu, China. All captured lizards were transported to our laboratory at Nanjing Normal University. Individuals were housed in cages with a substrate of moist sand (200-mm depth). We used Dufaure and Hubert's (61) embryonic stage scheme to identify embryonic stage in both species. We sampled at six developmental stages for *P. vlangalii* [S1 (ovarian egg period), S2 (stages 25–26), S3 (stages 30–31), S4 (stages 35–36), S5 (late stage 40, up to birth), and S6 (24 h after litter release)], and at four stages for *P. przewalskii* [S1 (ovarian egg period), S2 (stages 25–26), S3 (stages 30–31, soon before egg-laying), and S4 (24 h after egg-laying)]. We sampled five individuals at each stage. Lizards were killed by decapitation when they were at the targeted stages mentioned above. Oviduct/uteri were excised and submerged in RNAlater before being stored at 4 °C overnight, and then stored at −80 °C.

RNA Sequencing and Expression Abundance Calculation. Total RNA was extracted using TRIzol reagent (Invitrogen) and RNeasy Mini Kit (Qiagen). RNA integrity was assessed using the RNA Nano 6000 Assay Kit of the Agilent Bioanalyzer 2100 system (Agilent Technologies). All of the RNA libraries were sequenced through Illumina HisEq 4000 platform (with read length of 150 bp). All clean reads were mapped to the reference genomes of *P. vlangalii* and *P. przewalskii* using HISAT2 (62). We then calculated the transcript abundances used StringTie (62, 63) with the parameters of "-A -eB". Additional details are given in *SI Appendix*.

Expression Pattern Visualization and DEGs. For all of the ortholog genes and samples in the two species, their expression values, in terms of fragments per kilobase million, were used as the input for PCA. EdgeR (64) was used to identify DEGs of all pairwise comparisons of the sampled time periods in *P. vlangalii* and *P. przewalskii*, respectively. The Benjamini–Hochberg method (65) was used to correct for multiple testing; genes with an FDR < 0.05 and log-transformed fold change (logFC) > 1 were considered to be DEGs.

WGCNA and Functional Enrichment. The WGCNA (66) package was used to perform WGCNA, using the unsigned correlation as option and setting the minimum cluster size to 50 members. The Benjamini–Hochberg method (65) was used to correct for multiple testing when calculating the correlation between modules and stages. GO term enrichment analyses on gene sets were performed using the GOseq package (67) and Blast2GO (68). Significant GO terms identified by both methods were retained for further analysis. We used the java package GSEA (69) to find significantly enriched Kyoto Encyclopedia of Genes and Genomes pathways. *P* values were estimated using permutation tests, with FDRs calculated (69).

Convergence and Positive Selection of Genes Associated with Viviparity. To explore the convergence of viviparity in lizards, we sequenced the transcriptome of other three oviparous/viviparous pairs of species of the genera *Eremias*, *Scincella*, and *Sphenomorphus* (Fig. 4*A*). Tissues (heart, liver, lung, muscle, brain, oviduct) of each species were obtained and RNA extraction was performed as described above. A single pooled RNA sample was prepared for each species by mixing equal volumes of the RNA extracted from each tissue sample. Library preparation and sequencing were the same as that described above. De novo assembly for each species was generated by Trinity (70) with its default parameters. A modified Reciprocal Best Hit method (71) was used to calculate ortholog genes with high accuracy. All of the orthologs identified were concatenated into a "super-gene" alignment by FasParser (72), which was then used as input to infer a phylogeny by using RAxML v7.3.5 with the "GTRGAMMA" model of evolution (73).

Based on the orthologous genes, we analyzed convergent amino acid replacements using the methods described in Foote et al. (53). Briefly, all orthologous gene alignments were trimmed and then translated to amino acid alignments with FasParser (72). The codeml program (74) was then used for reconstruction of ancestral sequences under the accepted phylogenetic tree. For each of the four viviparous lizards—*Eremias multiocellata*, *P. vlangalii*, *Scincella reevesii*, *Sphenomorphus indicus*—the extant sequences at each position were compared with oviparous relative species and the ancestral sequence at the node corresponding to the most recent ancestor. The ancestral nodes are those at the roots of the red branches in Fig. 4*A*. We identified amino acid positions for which replacements were inferred to have occurred and shared by all four species. Because viviparous species in different environments may experience different selective forces, the transition of oviparity to viviparity may be accomplished via different amino acid replacements at the same position. Therefore, identical and nonidentical amino acid replacements were both considered as potential convergent events.

To test whether the levels of observed convergence were greater than expected by chance, we applied the evolver program (74) to simulate the gene sequences under the observed tree topology, which exhibited the same number, length, and level of divergence as all ortholog genes observed. The terminal branch sequences were then used to examine the level of expected random convergence in the four viviparous lineages. This analysis was repeated 1,000 times. We then compared the distribution of convergent level in simulated sequences to that observed in the actual genes ($n = 4$) (Fig. 5*B*), and calculated the frequency of convergence in at least four genes among the 1,000 simulations.

In addition, evolutionary convergence in rate shift among the four viviparous species was assessed using the methods described in Chikina et al. (54). We estimated branch lengths for each amino acid alignment using aaml (74). Raw branch lengths were transformed into relative rates using a projection operator method (75). Then we determine the relative rate of each branch as the residual of that branch after factoring out the normalization vector. We used these branch-specific relative rates to perform a Wilcoxon rank sum test and correlation analysis over the binary variable of "oviparous" or "viviparous" branches. Correction for multiple tests used q-value methods described in Chikina et al. (54).

Positive selection of genes that occurred in the viviparous *P. vlangalii* after its split from *P. przewalskii* were detected according to the branch-site model (76). Details of these analyses are in *SI Appendix*.

Identity of Candidate Genes Related to Viviparity Evolution. To identify genes related to shell gland formation, we identified HEGs at S1 (compared with any other stages) in *P. przewalskii*. For comparison, the HEGs at S1 in *P. vlangalii* were also calculated using the same methods. HEGs were identified from DEGs calculated by edgeR.

To identify genes related to placentation and embryo attachment, we evaluated the genes that were highly expressed at midperiods of gestation in *P. vlangalii*. There were six patterns of gene expression, which we labeled as patterns P1–P6, as follows: P1, genes highly expressed at S2, S3, and S4 compared with S1, S5, and S6; P2, genes highly expressed at S2 and S3 compared with S1, S5, and S6; P3, genes highly expressed at S3 and S4 compared with S1, S5, and S6; P4, genes highly expressed at S2 compared with S1, S5, and S6; P5, genes highly expressed at S3 compared with S1, S5, and S6; P5, genes highly expressed at S3 compared with S1, S5, and S6; and P6, genes highly expressed at S4 compared with S1, S5, and S6. For genes

related to placental development and embryo attachment, we expected the ortholog genes in *P. przewalskii* to not be up-regulated after pregnancy. Thus, genes whose orthologs in *P. przewalskii* were highly expressed at S2 or S3 (compared with S1) were removed from further analysis.

Samples Collecting Permit and Animal Welfare. Permission for field surveys was granted by the Forestry Department and National Reserves of China. Collecting permit (BBCJ-2014-001) was issued by the Chinese Academy of Sciences. Animal welfare regulations of the Kunming Institute of Zoology and Nanjing Normal University were followed for proper treatment of animals.

ACKNOWLEDGMENTS. We thank Qiang Chen (Lanzhou University), Chung-I Wu (Sun Yat-sen University), Guo-Dong Wang (Kunming Institute of Zoology, Chinese Academy of Sciences), Min-Sheng Peng (Kunming Institute of Zoology, Chinese Academy of Sciences), and Qi Zhou (Zhejiang University) for helpful comments and suggestions; Kai Wang (University of Oklahoma) for providing and edits of lizard photos; and Yan-Qing Wu and Kun Guo (Nanjing Normal University) for their help with animal feeding and sample collection. This research was supported by Strategic Priority Research Program (B) Grant XDB13020200 of the Chinese Academy of Sciences; National Key Research and Development Program of China Grant 2017YFC0505202; National Natural Science Foundation of China Grants 91431105, 31671326, 31672277, 31470471, and 31670422; and the Animal Branch of the Germplasm Bank of Wild Species of Chinese Academy of Sciences (the Large Research Infrastructure Funding). J.C., Y.-B.S., and W.-W.Z. were supported by the Youth Innovation Promotion Association, Chinese Academy of Sciences. Y.-B.S. was also supported by Chinese Academy of Sciences "Light of West China" Program. D.M.H. was funded by Chinese Academy of Sciences President's International Fellowship Initiative, Grant 2018VBA0039.

1. Stewart JR, Blackburn DG (2014) Viviparity and placentation in lizards. *Reproductive Biology and Phylogeny of Lizards and Tuatara*, eds Rheubert JL, Siegel DS, Trauth SE (CRC Press, Boca Raton, FL), pp 448–563.
2. Blackburn DG (2000) Classification of the reproductive patterns of amniotes. *Herpetol Monogr* 14:371–377.
3. Blackburn DG (2006) Squamate reptiles as model organisms for the evolution of viviparity. *Herpetol Monogr* 20:131–146.
4. Blackburn DG (2015) Evolution of vertebrate viviparity and specializations for fetal nutrition: A quantitative and qualitative analysis. *J Morphol* 276:961–990.
5. Wright AM, Lyons KM, Brandley MC, Hillis DM (2015) Which came first: The lizard or the egg? Robustness in phylogenetic reconstruction of ancestral states. *J Exp Zoolog B Mol Dev Evol* 324:504–516.
6. Blackburn DG (1999) Are viviparity and egg-guarding evolutionarily labile in squamates? *Herpetologica* 55:556–573.
7. Fenwick AM, Greene HW, Parkinson CL (2012) The serpent and the egg: Unidirectional evolution of reproductive mode in vipers? *J Zool Syst Evol Res* 50:59–66.
8. Lynch VJ, Wagner GP (2010) Did egg-laying boas break Dollo's law? Phylogenetic evidence for reversal to oviparity in sand boas (*Eryx*: Boidae). *Evolution* 64:207–216.
9. King B, Lee MSY (2015) Ancestral state reconstruction, rate heterogeneity, and the evolution of reptile viviparity. *Syst Biol* 64:532–544.
10. Heulin B, et al. (2005) Development of the uterine shell glands during the preovulatory and early gestation periods in oviparous and viviparous *Lacerta vivipara*. *J Morphol* 266:80–93.
11. Packard GC, Tracy CR, Roth JJ (1977) The physiological ecology of reptilian eggs and embryos, and the evolution of viviparity within the class reptilia. *Biol Rev Camb Philos Soc* 52:71–105.
12. Guillette LJ (1993) The evolution of viviparity in lizards. *Bioscience* 43:742–751.
13. Thompson MB, Speake BK (2006) A review of the evolution of viviparity in lizards: Structure, function and physiology of the placenta. *J Comp Physiol B* 176:179–189.
14. Murphy BF, Thompson MB (2011) A review of the evolution of viviparity in squamate reptiles: The past, present and future role of molecular biology and genomics. *J Comp Physiol B* 181:575–594.
15. Guillette LJ, Jr, Jones RE (1985) Ovarian, oviductal, and placental morphology of the reproductively bimodal lizard, *Sceloporus aeneus*. *J Morphol* 184:85–98.
16. Thompson MB, Stewart JR, Speake BK (2000) Comparison of nutrient transport across the placenta of lizards differing in placental complexity. *Comp Biochem Physiol A Mol Integr Physiol* 127:469–479.
17. Van Dyke JU, Brandley MC, Thompson MB (2013) The evolution of viviparity: Molecular and genomic data from squamate reptiles advance understanding of live birth in amniotes. *Reproduction* 147:R15–R26.
18. Graham SP, Earley RL, Guyer C, Mendonça MT (2011) Innate immune performance and steroid hormone profiles of pregnant versus nonpregnant cottonmouth snakes (*Agkistrodon piscivorus*). *Gen Comp Endocrinol* 174:348–353.
19. Hendrawan K, Whittington CM, Brandley MC, Belov K, Thompson MB (2017) The regulation of uterine proinflammatory gene expression during pregnancy in the live-bearing lizard, *Pseudemoia entrecasteauxii*. *J Exp Zoolog B Mol Dev Evol* 328:334–346.
20. Cornetti L, et al. (2018) Candidate genes involved in the evolution of viviparity: A RAD sequencing experiment in the lizard *Zootoca vivipara* (Squamata: Lacertidae). *Zool J Linn Soc* 183:196–207.
21. Brandley MC, Young RL, Warren DL, Thompson MB, Wagner GP (2012) Uterine gene expression in the live-bearing lizard, *Chalcides ocellatus*, reveals convergence of squamate reptile and mammalian pregnancy mechanisms. *Genome Biol Evol* 4: 394–411.
22. Griffith OW, Brandley MC, Belov K, Thompson MB (2016) Reptile pregnancy is underpinned by complex changes in uterine gene expression: A comparative analysis of the uterine transcriptome in viviparous and oviparous lizards. *Genome Biol Evol* 8: 3226–3239.
23. Pang J, et al. (2003) A phylogeny of Chinese species in the genus *Phrynocephalus* (Agamidae) inferred from mitochondrial DNA sequences. *Mol Phylogenet Evol* 27: 398–409.
24. Solovyeva EN, et al. (2018) Cenozoic aridization in Central Eurasia shaped diversification of toad-headed agamas (*Phrynocephalus*; Agamidae, Reptilia). *PeerJ* 6: e4543.
25. Simão FA, Waterhouse RM, Ioannidis P, Kriventseva EV, Zdobnov EM (2015) BUSCO: Assessing genome assembly and annotation completeness with single-copy orthologs. *Bioinformatics* 31:3210–3212.
26. Guillette LJ (1987) The evolution of viviparity in fishes, amphibians and reptiles: An endocrine approach. *Hormones and Reproduction in Fishes, Amphibians, and Reptiles*, eds Norris DO, Jones RE (Plenum Press, New York), pp 523–562.
27. Albergotti LC, Guillette LJ, Jr (2011) Viviparity in reptiles: Evolution and reproductive endocrinology. *Hormones and Reproduction of Vertebrates*, eds Norris DO, Lopez KH (Academic, San Diego), pp 247–275.
28. Girling JE (2002) The reptilian oviduct: A review of structure and function and directions for future research. *J Exp Zool* 293:141–170.
29. Stewart JR, Blackburn DG (1988) Reptilian placentation: Structural diversity and terminology. *Copeia* 1988:839–852.
30. Adams SM, Biazik J, Stewart RL, Murphy CR, Thompson MB (2007) Fundamentals of viviparity: Comparison of seasonal changes in the uterine epithelium of oviparous and viviparous *Lerista bougainvillii* (Squamata: Scincidae). *J Morphol* 268:624–635.
31. Adams SM, Lui S, Jones SM, Thompson MB, Murphy CR (2007) Uterine epithelial changes during placentation in the viviparous skink *Eulamprus tympanum*. *J Morphol* 268:385–400.
32. Paulesu L, et al. (2001) Evidence of H β 58, a gene involved in mammalian placental development, in the three-toed skink, *Chalcides chalcides* (Squamata: Scincidae), a viviparous placentotrophic reptile. *Placenta* 22:735–741.
33. Wu Q, Thompson MB, Murphy CR (2011) Changing distribution of cadherins during gestation in the uterine epithelium of lizards. *J Exp Zoolog B Mol Dev Evol* 316: 440–450.
34. Mason RW (2008) Emerging functions of placental cathepsins. *Placenta* 29:385–390.
35. Kretz M, et al. (2013) Control of somatic tissue differentiation by the long non-coding RNA TINCR. *Nature* 493:231–235.
36. Sonderegger S, Pollheimer J, Knöfler M (2010) Wnt signalling in implantation, decidualisation and placental differentiation—Review. *Placenta* 31:839–847.
37. Yuan J, et al. (2016) Planar cell polarity signaling in the uterus directs appropriate positioning of the crypt for embryo implantation. *Proc Natl Acad Sci USA* 113: E8079–E8088.
38. Fujimoto J, et al. (2005) Estrogen-related receptor expression in placenta throughout gestation. *J Steroid Biochem Mol Biol* 94:67–69.
39. Guillette LJ, Jr, et al. (1997) The reproductive cycle of the female American alligator (*Alligator mississippiensis*). *Gen Comp Endocrinol* 108:87–101.
40. Huet-Hudson YM, et al. (1990) Estrogen regulates the synthesis of epidermal growth factor in mouse uterine epithelial cells. *Mol Endocrinol* 4:510–523.
41. Edwards A, Jones SM (2001) Changes in plasma progesterone, estrogen, and testosterone concentrations throughout the reproductive cycle in female viviparous blue-tongued skinks, *Tiliqua nigrolutea* (Scincidae), in Tasmania. *Gen Comp Endocrinol* 122:260–269.
42. Paolucci M, Di Fiore MM (1994) Estrogen and progesterone receptors in lizard *Podarcis s. sicula* oviduct: Seasonal distribution and hormonal dependence. *J Exp Zool* 269:432–441.
43. Atkins N, Jones SM, Guillette LJ, Jr (2006) Timing of parturition in two species of viviparous lizard: Influences of β-adrenergic stimulation and temperature upon uterine responses to arginine vasotocin (AVT). *J Comp Physiol B* 176:783–792.
44. Guillette LJ, Jr, DeMarco V, Palmer BD, Masson GR (1992) Effects of arachidonic acid, prostaglandin $F_{2\alpha}$, prostaglandin E_2, and arginine vasotocin on induction of birth in vivo and in vitro in a viviparous lizard (*Sceloporus jarrovi*). *Gen Comp Endocrinol* 85: 477–485.
45. Guillette LJ, Jr, Masson GR, DeMarco V (1991) Effects of prostaglandin $F_{2\alpha}$ prostaglandin E_2 and arachidonic acid on the induction of oviposition in vivo and *in vitro* in oviparous lizards. *Prostaglandins* 42:533–540.
46. Guillette LJ, Propper CR, Cree A, Doresl RM (1991) Endocrinology of oviposition in the tuatara (*Sphenodon punctatus*)-II. Plasma arginine vasotocin concentrations during natural nesting. *Comp Biochem Physiol Part A Physiol* 100:819–822.
47. Arrowsmith S, Wray S (2014) Oxytocin: Its mechanism of action and receptor signalling in the myometrium. *J Neuroendocrinol* 26:356–369.
48. Fergusson B, Bradshaw SD (1991) Plasma arginine vasotocin, progesterone, and luteal development during pregnancy in the viviparous lizard *Tiliqua rugosa*. *Gen Comp Endocrinol* 82:140–151.
49. Guillette LJ, Jones RE (1982) Further observations on arginine vasotocin-induced oviposition and parturition in lizards. *J Herpetol* 16:140–144.
50. Smith WL, DeWitt DL, Garavito RM (2000) Cyclooxygenases: Structural, cellular, and molecular biology. *Annu Rev Biochem* 69:145–182.

51. Cree A, Guillette LJ, Jr (1991) Effect of β-adrenergic stimulation on uterine contraction in response to arginine vasotocin and prostaglandin $F_{2\alpha}$ in the gecko *Hoplodactylus maculatus*. *Biol Reprod* 44:499–510.
52. Fleming JGW, Spencer TE, Safe SH, Bazer FW (2006) Estrogen regulates transcription of the ovine oxytocin receptor gene through GC-rich SP_1 promoter elements. *Endocrinology* 147:899–911.
53. Foote AD, et al. (2015) Convergent evolution of the genomes of marine mammals. *Nat Genet* 47:272–275.
54. Chikina M, Robinson JD, Clark NL (2016) Hundreds of genes experienced convergent shifts in selective pressure in marine mammals. *Mol Biol Evol* 33:2182–2192.
55. Castaño AP, et al. (2009) Serum amyloid P inhibits fibrosis through Fc γ R-dependent monocyte-macrophage regulation in vivo. *Sci Transl Med* 1:5ra13.
56. Girardi G, Bulla R, Salmon JE, Tedesco F (2006) The complement system in the pathophysiology of pregnancy. *Mol Immunol* 43:68–77.
57. Li L, et al. (2012) A peripheral blood diagnostic test for acute rejection in renal transplantation. *Am J Transplant* 12:2710–2718.
58. Sowerby JM, et al. (2017) NBEAL2 is required for neutrophil and NK cell function and pathogen defense. *J Clin Invest* 127:3521–3526.
59. Kajitani R, et al. (2014) Efficient de novo assembly of highly heterozygous genomes from whole-genome shotgun short reads. *Genome Res* 24:1384–1395.
60. Emms DM, Kelly S (2015) OrthoFinder: Solving fundamental biases in whole genome comparisons dramatically improves orthogroup inference accuracy. *Genome Biol* 16: 157.
61. Dufaure JP, Hubert J (1961) Table de développement du lézard vivipare: *Lacerta* (*Zootoca*) *vivipara* Jacquin. *Arch Anat Microsc Morphol Exp* 50:309–328.
62. Pertea M, Kim D, Pertea GM, Leek JT, Salzberg SL (2016) Transcript-level expression analysis of RNA-seq experiments with HISAT, StringTie and Ballgown. *Nat Protoc* 11: 1650–1667.
63. Pertea M, et al. (2015) StringTie enables improved reconstruction of a transcriptome from RNA-seq reads. *Nat Biotechnol* 33:290–295.
64. Robinson MD, McCarthy DJ, Smyth GK (2010) edgeR: A bioconductor package for differential expression analysis of digital gene expression data. *Bioinformatics* 26: 139–140.
65. Benjamini Y, Hochberg Y (1995) Controlling the false discovery rate: A practical and powerful approach to multiple testing. *J R Stat Soc B* 57:289–300.
66. Langfelder P, Horvath S (2008) WGCNA: An R package for weighted correlation network analysis. *BMC Bioinformatics* 9:559.
67. Young MD, Wakefield MJ, Smyth GK, Oshlack A (2010) Gene ontology analysis for RNA-seq: Accounting for selection bias. *Genome Biol* 11:R14.
68. Conesa A, et al. (2005) Blast2GO: A universal tool for annotation, visualization and analysis in functional genomics research. *Bioinformatics* 21:3674–3676.
69. Subramanian A, et al. (2005) Gene set enrichment analysis: A knowledge-based approach for interpreting genome-wide expression profiles. *Proc Natl Acad Sci USA* 102: 15545–15550.
70. Grabherr MG, et al. (2011) Full-length transcriptome assembly from RNA-seq data without a reference genome. *Nat Biotechnol* 29:644–652.
71. Aubry S, Kelly S, Kümpers BMC, Smith-Unna RD, Hibberd JM (2014) Deep evolutionary comparison of gene expression identifies parallel recruitment of trans-factors in two independent origins of C_4 photosynthesis. *PLoS Genet* 10:e1004365.
72. Sun Y-B (2017) FasParser: A package for manipulating sequence data. *Zool Res* 38: 110–112.
73. Stamatakis A (2006) RAxML-VI-HPC: Maximum likelihood-based phylogenetic analyses with thousands of taxa and mixed models. *Bioinformatics* 22:2688–2690.
74. Yang Z (2007) PAML 4: Phylogenetic analysis by maximum likelihood. *Mol Biol Evol* 24:1586–1591.
75. Sato T, Yamanishi Y, Kanehisa M, Toh H (2005) The inference of protein-protein interactions by co-evolutionary analysis is improved by excluding the information about the phylogenetic relationships. *Bioinformatics* 21:3482–3489.
76. Zhang J, Nielsen R, Yang Z (2005) Evaluation of an improved branch-site likelihood method for detecting positive selection at the molecular level. *Mol Biol Evol* 22: 2472–2479.